1-1-2006

The Flagellar Motility of *Chlamydomonas pf25* Mutant Lacking an AKAP-binding Protein Is Overtly Sensitive to Medium Conditions

Chun Yang
Marquette University

Pinfen Yang
Marquette University, pinfen.yang@marquette.edu

Published version. *Molecular Biology of the Cell*, Vol. 17, No. 1 (January 2006): 227-238. DOI.

Molecular Biology of the Cell
Vol. 17, 227–238, January 2006

The Flagellar Motility of *Chlamydomonas pf*25 Mutant Lacking an AKAP-binding Protein Is Overtly Sensitive to Medium Conditions[V]

Chun Yang and Pinfen Yang

Department of Biological Sciences, Marquette University, Milwaukee WI 53233

Submitted July 14, 2005; Revised October 17, 2005; Accepted October 25, 2005
Monitoring Editor: Yixian Zheng

Radial spokes are a conserved axonemal structural complex postulated to regulate the motility of 9 + 2 cilia and flagella via a network of phosphoenzymes and regulatory proteins. Consistently, a *Chlamydomonas* radial spoke protein, RSP3, has been identified by RII overlays as an A-kinase anchoring protein (AKAP) that localizes the cAMP-dependent protein kinase (PKA) holoenzyme by binding to the RIIa domain of PKA RII subunit. However, the highly conserved docking domain of PKA is also found in the N termini of several AKAP-binding proteins unrelated to PKA as well as a 24-kDa novel spoke protein, RSP11. Here, we report that RSP11 binds to RSP3 directly in vitro and colocalizes with RSP3 toward the spoke base near outer doublets and dynein motors in axonemes. Importantly, RSP11 mutant *pf*25 displays a spectrum of motility, from paralysis with flaccid or twitching flagella as other spoke mutants to wild-typelike swimming. The wide range of motility changes reversibly depending on the condition of liquid media without replacing defective proteins. We postulate that radial spokes use the RIIa/AKAP module to regulate ciliary and flagellar beating; absence of the spoke RIIa protein exposes a medium-sensitive regulatory mechanism that is not obvious in wild-type *Chlamydomonas*.

INTRODUCTION

The oscillatory beating of 9 + 2 cilia and flagella is tightly regulated (reviewed by Smith and Yang, 2004). However, the molecular basis of the regulation remains to be elucidated. *Chlamydomonas* mutants have been invaluable to address this challenge with unique approaches. Mutations in genes encoding dynein motors and the adjacent dynein regulatory complex suppress the paralysis of mutants defective in radial spokes or central pair, leading to the hypothesis that central pair and radial spokes constitute a system that controls the dynein-driven motility (Huang *et al*., 1982). The control system may determine the preferential sliding among the nine outer doublets (Mitchell, 2003; Wargo and Smith, 2003) and is involved in motility changes mediated by second messengers and phosphoenzymes (reviewed by Porter and Sale, 2000). In particular, cAMP-dependent protein kinase (PKA) and calcium/calmodulin-dependent protein kinases are anchored to axonemes, and the heightened kinase activities in the mutant axonemes are correlated with paralyzed flagella and inhibited motor activities (Howard *et al*., 1994; Habermacher and Sale, 1997; King and Dutcher, 1997; Smith, 2002; Hendrickson *et al*., 2004).

The coupling of second messengers, phosphoenzymes, and the control system is further illuminated by the identification of two A-kinase anchoring proteins (AKAPs), one each at radial spokes and central pair apparatus, by a comprehensive RII overlay (Gaillard *et al*., 2001). This well established method using RII, the regulatory subunit of PKA as a probe, is credited for identifying numerous AKAPs (Bregman *et al*., 1989; reviewed by Pawson and Scott, 2005) that dock PKA as well as other signaling molecules along the molecular scaffolds, possibly for specific and integrated regulation (Dell'Acqua *et al*., 2002; Malbon *et al*., 2004; reviewed by Wong and Scott, 2004). Anchoring of PKA, the central tenant of AKAPs, is achieved by the hydrophobic association of an amphipathic region in AKAPs with RIIa domain at the N terminus of RII.

The spoke AKAP that the RII probe binds to is radial spoke protein (RSP) 3, ideally located at the base of radial spoke for anchoring the structural complex to outer doublets (Diener *et al*., 1993) and near dynein motors and presumably for targeting PKA regulatory pathways as well. The simplest interpretation is that RSP3 directs the cAMP-sensitive holoenzymes near dynein motors to locally change ciliary and flagellar motility (Gaillard *et al*., 2001).

However, in addition to PKA RII, certain AKAPs may interact with non-RII proteins that share the RIIa domain known for dimerization and docking to AKAPs via hydrophobic interaction (Newlon *et al*., 2001). A domain similar to RIIa is present in RI, an isoform of RII and binds the amphipathic helix of AKAPs as well, albeit at a lower affinity (Banky *et al*., 2000). Phenotypes of RI and RII knockout mice reveal distinct functions of RI and RII (reviewed by Amieux and McKnight, 2002). Most intriguingly, inhibitors of PKA enzymatic activity and the peptides that perturb the anchorage of the regulatory subunit affect sperm flagellar motility differently (Vijayaraghavan *et al*., 1997). These findings suggest that the functions of some AKAPs, at least in mammalian sperm, are independent to RII or PKA.

This prediction is substantiated by the finding of non-PKA proteins that contain an RIIa domain at their N termini. ASP, ropporin, CABYR, and SP17 are abundant in testis, sperm, and the flagellar compartment and bind sperm AKAPs in

This article was published online ahead of print in *MBC in Press* (http://www.molbiolcell.org/cgi/doi/10.1091/mbc.E05–07–0630) on November 2, 2005.

[V] The online version of this article contains supplemental material at *MBC Online* (http://www.molbiolcell.org).

Address correspondence to: Pinfen Yang (pinfen.yang@marquette.edu).

vitro (Carr *et al*., 2001; Naaby-Hansen *et al*., 2002; Lea *et al*., 2004; reviewed by Eddy *et al*., 2003). Intriguingly, they do not contain the signature cAMP-binding domains that mediate cAMP-dependent allosteric regulation of the holoenzyme. Rather, yeast two-hybrid system shows that the C terminus of ropporin associates with rhophilin (Fujita *et al*., 2000), a Rho-binding protein postulated to be a cytoskeletal target protein for the small GTPase (Nakamura *et al*., 1999), whereas CABYR and SP17 contains calcium-signaling related modules (Richardson, 1994; Naaby-Hansen *et al*., 2002). The physiological partners and functions of these non-PKA RIIa proteins remains to be established.

Given the presence of multiple RIIa proteins, particularly in flagella, it is central to determine experimentally the physiological binding partner of the spoke AKAP to elucidate the functional mechanism of radial spokes and the spoke AKAP. Recently, a systematic characterization of new spoke proteins revealed that the 24-kDa RSP11 is a non-PKA RIIa protein (submission). The RSP11 mutant *pf*25 has been identified previously by dikaryon rescue that cytoplasmic components from wild-type cells complement the mutant gene product in mating heterozygotes (Huang *et al*., 1981). *Pf*25 is unique compared with the other spoke mutants that the assembly of the macromolecular complex is affected leading to deficiency of multiple spoke proteins, gross morphological defect and paralyzed flagella. In contrast, *pf*25 lacks the 24-kDa RSP11 and has reduced amount of the 40-kDa RSP8, whereas the ultrastructure and protein composition are largely unaffected. Importantly, *pf*25 described as swimming actively but in an abnormal manner provides a rare opportunity to study the functional mechanism of the non-PKA RIIa protein and radial spokes. Here, we describe the cloning of RSP11 gene and present both in vitro and in vivo evidence suggesting that radial spokes use non-PKA RIIa/AKAP module for the control of ciliary and flagellar beating.

MATERIALS AND METHODS

Strains and Culture Conditions

Chlamydomonas reinhardtii strains used in this report include wild-type strains [cc124(−), cc125(+), cc620(+), and cc621(−)]; the defined radial spoke mutants *pf14*, *pf17*, *pf24* and the available *pf25* alleles *pf*25(+),*pf*25(−) *pf*25A *pf*25D *pf*25F (Huang *et al*., 1981); and the central pair mutants *pf6* and *pf19*. These strains are acquired from the *Chlamydomonas* Genetics Center (Duke University, Durham, NC). The *pf*28*pf*30 strain lacks both the 20S outer arm dynein and inner arm dynein I1 as described previously (Piperno *et al*., 1990) and was used for purification of 20S wild-type radial spokes. All cells were grown in liquid modified medium I under aerated photoheterotrophic growth condition and a 14/10 light/dark cycle (Witman, 1986).

Biochemistry

Axonemal Fractionation. Preparation of axonemes and KI axonemal extract; velocity sedimentation of KI extract on sucrose gradients and two-dimensional (2-D) electrophoresis of nonequilibrium isoelectric focusing followed by SDS-PAGE (nonequilibrium pH gel electrophoresis) were carried out as described previously (Yang *et al*., 2001). Blue native-PAGE was performed as described previously (Yang *et al*., 2005) except that 5–10% gradient gel was used, and electrophoresis in the cathode buffer was increased to ~6 h. For further separation in SDS-PAGE, the blue native gel lanes were excised and then immersed in 5× SDS-PAGE sample buffer for 30 min at room temperature for protein denaturation. Subsequently, the top part of each gel strip containing the spoke particles was inserted into a preparatory mini-gel for standard SDS-PAGE and Western Blot.

Overlays. Overlays were performed as described previously (Gaillard *et al*., 2001) with modification to detect the bound ligands indirectly by enhanced chemiluminescence as Western blot (Yang *et al*., 2005). Briefly, nitrocellulose membrane blotted with 10 μg of axoneme proteins was blocked with 5% milk in Tris-buffered saline (TBS) for 30 min at room temperature and 10 min at 40°C. Four microliters of Ni-NTA purified RSP11–6 His (2 mg/ml) was overlaid on the membrane in 10 ml of blocking solution for 20 min at 40°C and 1 h at 37°C. After three 5-min washes with TBS, the membrane were further incubated with mouse anti-6 His antibody (QIAGEN, Valencia, CA) for 2 h at 37°C and then horseradish peroxidase-tagged secondary antibodies for 1 h at room temperature.

Molecular Biology and Genetics

Reverse transcription of *Chlamydomonas* poly(A) RNA was carried out using the Oligo(dT) primer and SuperScript II polymerase as suggested by the manufacturer (Invitrogen, Carlsbad, CA). The subsequent PCR was amplified by *pf*u (Stratagene, La Jolla, CA) using the primer pair with built-in *Nco*I and *Eco*RI sites (underlined), catgccatggacgtggagccaatctt and antisense ggaattctcagacagccccagcttggg. The 0.6-kb product was cloned into pGEM-Teasy vector (Promega, Madison, WI), and the identity was confirmed by sequencing. The insert was directionally ligated into the respective restriction sites in pET28(a) (Novagen, Madison, WI) expression vector that carries kanamycin-resistant gene. Plasmid construct for glutathione *S*-transferase (GST)-RSP3 expression under the selection of ampicillin was as described previously (Gaillard *et al*., 2001). The expression constructs for tagged RSP11 alone or for both proteins were transformed into bacteria BL21(DE3) under single- or double-antibiotic selection. The isopropyl β-D-thiogalactoside (IPTG)-induced expression and Ni-NTA purification under nature condition were carried out as described previously (Yang *et al*., 2005).

Secondary structure and domains were predicted by the Web-available programs PHD (Rost and Sander, 1993; http://pbil.univ-lyon1.fr/) and SMART (Letunic *et al*., 2004; http://smart.embl-heidelberg.de/) with default parameters. The BLAST server at National Center for Biotechnology Information was used to search nucleotide and protein databases for RSP11 homologues.

Transformation Rescue. *Pf*25 cells were cotransformed with genomic DNA and plasmid pSI103 that confers paromomycin resistance (*Chlamydomonas* Genetics Center) using glass bead method as described previously (Nguyen *et al*., 2005) with minor modification. DNA of *Chlamydomonas* genomic BAC clone #1L24 (Clemson University, Clemson, SC) was purified using PhasePrep BAC DNA kit (Sigma-Aldrich, St. Louis, MO). A 7-kb fragment released from the BAC DNA by *Not*I digest was cloned into pBlueScript II KS (Stratagene). The subclone containing RSP11 gene was confirmed by restriction digest and PCR. For transformation, *pf*25 cells were treated with autolysin at 1×10^7 cells/ml for 1–2 h until ~50% cell lyses by 0.5% NP-40 treatment. Cells were gently spun down and resuspended in TAP medium at 1×10^8 cell/ml (Harris, 1988). One microgram of *Not*I subclone plasmid (or ~5 μg of BAC DNA), 0.5 μg of pSI103 (*Chlamydomonas* Genetics Center), 300 μg of glass beads, and 100 μl of 20% PEG 8000 were added into 0.3 ml of cells, and the mixture was vortexed at speed 8 (Mini-Vortexer; VWR, West Chester, PA) for 45 s. The cell supernatant was removed after addition of 10 ml of TAP medium. Cell pellets were resuspended in 5 ml of TAP medium, shaken gently under bright light for 24 h, and then plated on paromomycin (10 μg/ml)/TAP plates. Colonies forming in 4–5 d were streaked on TAP plates for motility evaluation under light microscope.

Backcross. Mating and tetrad analysis of *pf*25(−) cells with wild type strain cc125(+) were carried out as described previously (Harris, 1988, pp. 171–173 and 419–432) except that the zygotic mixture was plated on 2.5% agar plate (A-7921; Sigma-Aldrich) for maturation and tetrad dissection.

Motility Assessment

The percentage of swimming cells was determined by observing cell culture placed in slide chambers with three layers of scotch tapes between slide and cover slide at 400× magnification with the Olympus compound microscope BH-2. Focal plane was centered between glass surfaces. Swimmers and cells with twitching flagella in random chosen fields were counted as separate categories. The cells that stuck to glass surface were not counted. Each of the data was derived from at least 500 cells from more than five randomly selected fields.

For imaging, cultured cells were observed at 400× magnification using Nikon Eclipse E600W compound microscope. The bright-field images were digitally captured using CoolSNAP-ES digital monochrome CCD camera (Photometrics, Tucson, AZ) and the stream mode of MetaMorph imaging system, version 6.1r5 (Molecular Devices, Sunnyvale, CA). For measurement of velocity, time-lapse images were taken at a rate of 10 frames/s for 20 s. Individual cell was tracked by MetaMorph software, and the mean velocity was derived from 20 to 30 individual swimming cells tracked from 25 to 30 sequential images at least. Statistical software program SPSS 10.0 for Windows (SPSS, Chicago, IL) was used to compare the velocities.

Antibodies

Anti-RSP11 and anti-RSP8 rabbit polyclonal antibodies were raised against Ni-NTA-purified recombinant RSP11–6 His and a synthetic cysteine tagged-RSP8 C-terminal peptide (C-DYRYHVDLPKFTPQAK). The rabbit antibodies against recombinant RSP16 and purified RSP3 from axoneme were described previously (Williams *et al*., 1989; Yang *et al*., 2005).

RESULTS

Identification of RSP11Gene

To study RSP11 and the intriguing phenotype of RSP11 mutant *pf*25, we first cloned the corresponding cDNA. The cloning strategy is illustrated in Figure 1A. RSP11 was spot purified from the 2-D gel of isolated radial spokes (Yang *et al*., 2001) and subjected to tandem mass spectrometry. The resulting two peptide sequences were used to identify expressed sequence tag (EST) clones available in the National Center of Biotechnology Information database and the gene in *Chlamydomonas* genome v.2, C_830019. Comparison of the overlapping EST clones and genomic sequence showed that the gene including the flanking untranslated region consists of five exons and four introns. The theoretical pI/molecular weight of the predicted protein is 4.5/21.5, consistent to RSP11 spot in 2-D gel (Piperno *et al*., 1981; Yang *et al*., 2001). PCR mapping using 3′ untranslated region (UTR) sequence indicated that RSP11 gene is located distal to molecular markers GP52 and CNA26 on linkage group X, as anticipated for *PF*25 (http://www.chlamy.org/BAC/LG10.htm; Kathir *et al*., 2003).

To confirm that *PF*25 encodes RSP11, transformation rescue of *pf*25 was carried out. First, BlastN search of BAC end sequences using RSP11 gene (C_830019) flanking sequences in scaffold _83 of *Chlamydomonas* genome v.2 (http://genome.jgi-psf.org/chlre2/chlre2.home.html) identified BAC clone #1L24 containing the entire RSP11 gene. Second, the purified BAC DNA was cotransformed into *pf*25A along with pSI103 that confers paromomycin resistance (Sizova *et al*., 2001). Among 74 antibiotic-resistant transformants, four displayed normal motility, in contrast to zero motility rescue among 96 colonies in the control group transformed with pSI103 only. A 7-kb *Not*I subclone that contains RSP11 gene with ~1.5- and 3-kb flanking sequences rescued *pf*25A as well as *pf*25(−) with 20 and 10% cotransformation rate, respectively (Figure 1B).

To independently test that the new protein is a radial spoke protein, recombinant protein was synthesized for raising antibodies. The coding sequence was amplified by reverse transcription (RT)-PCR and inserted in frame into the pET28(a) vector for the expression of a recombinant protein with a C-terminal 6-His tag. The construct was confirmed by restriction digestion and sequencing. The expression and purification were evaluated by Coomassie protein gel (Figure 1C, left). An abundant ~25-kDa His-tagged protein (arrowhead) was soluble in the IPTG-induced bacterial extract (pre) and was removed from the extract by Ni-affinity chromatography (post) and occurred in the imidazole elution butter (Elute). The polyclonal antibody raised against the recombinant protein recognized a 24-kDa band that was present in wild-type axonemes but absent in *pf*14 (Figure 1C, right; compare protein stain and Western of the same blot).

Sequencing the PCR products of ~3-kb RSP11 genomic DNA from *pf*25A revealed a G-to-A mutation in 5′ UTR (boxed letter in Figure 1D), resulting in a new out-of-frame ATG preceding the original translation initiation site (underlined M) and possible translation of a distinct polypeptide of 72 amino acids (bold letters). The mutation in *pf*25(−) seemed to occur in the middle of RSP11 genes because PCR fragments of N and C termini were normal, whereas the region between the third and fourth exons in *pf*25(−) or *pf*25(+) could not be amplified by either PCR or RT-PCR despite vigorous effort and correct primer sequences.

Sequence Analysis of RSP11 and RIIa Proteins

Motif search using Web-based SMART program (Letunic *et al*., 2004) revealed a RIIa domain at the N-terminal 11–53 aa of predicted RSP11 (Figure 2). Blastp homology search with default parameters revealed this region is highly homologous to the N terminus of the RII subunit of PKA as well as ~20-kDa proteins from diverse organisms such as the protozoan parasite *Giardia* (GL), *Caenorhabditis elegans* (CE), zebra fish (DR), and mammalians. The proteins from the last category include AKAP-binding sperm protein (ASP), ropporin (Fujita *et al*., 2000; Carr *et al*., 2001) as well as SP17 (Richardson *et al*., 1994). Homology of the predicted RSP11 with RI was not detected by Blastp. To illustrate the homology, the N-terminal sequences from representative proteins were aligned by Multiple Sequence Alignment and ClustalW (Figure 2A). The hallmark two helices in the RIIa domain (dashed underline) as well as the preceding β-strand (double underline) are based on NMR structural study of RII (Newlon *et al*., 2001). Consistently, PHD and other secondary structure prediction programs revealed a β-strand followed by helix-turn-helix in the N terminus of RSP11 (bold e and h, Figure 2B). Fourteen residues in RSP11 were identical or similar to the 19 aa of RII that are involved in dimerization and contacting AKAP (Figure 2A, asterisks and pound sign, respectively).

Among the RIIa proteins, the extreme N terminus of RSP11 was particularly homologous to ASP and the unknown fish and *Giardia* protein (arrow and overline, Figure 2A). Six of the nine residues were identical or similar, suggesting closer homology among the N termini of these four proteins. Sequence alignment of these proteins and ropporin showed that the proteins from vertebrates are homologous to each other largely through out the entire length of the molecules. However, the C termini of *Giardia* protein and RSP11 diverged significantly (Figure 2C).

Colocalization of RIIa Protein and AKAP in Radial Spokes

To test the association of RSP11 and RSP3, the RII-binding AKAP, we analyzed the axonemes of spoke mutants by Western blots. The spoke mutants *pf*14, *pf*24, and *pf*17 have different levels of structural and biochemical defects (Figure 3A), allowing localization of spoke proteins (Piperno *et al*., 1981; Yang *et al*., 2005; reviewed by Curry and Rosenbaum, 1993). Control antibodies for RSP3 and RSP16 (gray asterisks) confirmed the mutant strains. As anticipated, all three proteins were present in wild-type and central pair mutants *pf*6 and *pf*19 but absent in *pf*14. RSP11 was also absent in *pf*25, whereas RSP3 and RSP16 were normal (Figure 3B).

The detailed location of RSP11 is revealed by comparing RSP11 with RSP3 and RSP16 in *pf*24 (Figure 3, A and B). *Pf*24 had a polymorphic defect encompassing spokehead and the adjacent stalk area, but the basal end of the spokestalk was normal (Yang *et al*., 2005; Figure 3A) as reflected by normal RSP3 and diminished RSP16 (Figure 3B, arrowhead). As for spoke AKAP but unlike RSP16, RSP11 was present at wild-type level in *pf*24. To further test the colocalization, *pf*24 spokes were extracted by KI and fractionated by sucrose gradient velocity sedimentation. The peak spoke fraction was separated by native gel electrophoresis followed by 2-D SDS-PAGE and detected by Westerns. Compared with single intact spoke from dynein mutant (*pf*28*pf*30) and spokestalk from *pf*17, the polymorphic *pf*24 spoke particles revealed by RSP3 immunoblot were fractionated into three smaller particles (Yang *et al*., 2005). Importantly, RSP11 always colocalized with RSP3, including in the smallest par-

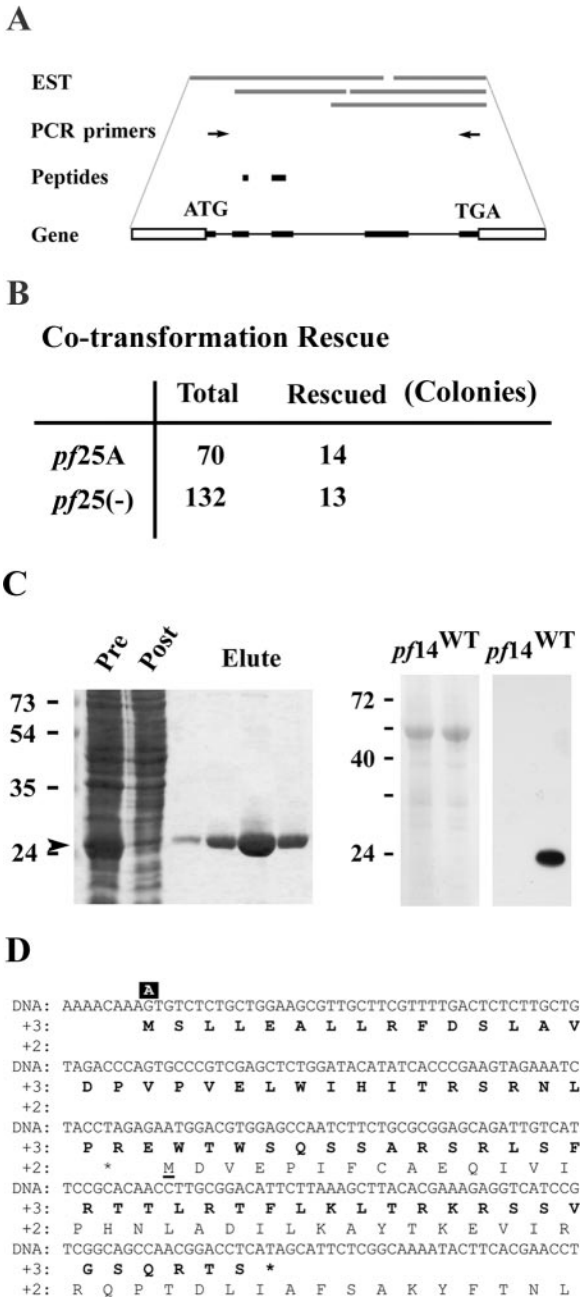

Figure 1. Identification of RSP11 gene and mutant. (A) Schematic picture depicts the strategy for identifying RSP11 gene and coding sequence. Searching EST database in National Center for Biotechnology Information and *Chlamydomonas* genome v.2. using the function of TBlastn and the two peptide sequences (solid bars) obtained by mass spectrometry identifies the corresponding and overlapping EST sequences (gray bars) and predicted gene C_830019 consisting of five exons and four introns. Untranslated regions in the first and last exons were represented by open bar. Primer pairs with sequences (arrows) at 5′ and 3′ end of the coding sequence are used in RT-PCR to amplify the region for creating a RSP11–6 His expression construct. (B) Rescue of two *pf*25 alleles by cotransformation with RSP11 genomic DNA in a 7-kDa *Not*I subclone plasmid and a plasmid conferring antibiotic resistance. (C) Antirecombinant protein recognizes a radial spoke protein of the size of RSP11. Coomassie blue gel shows purification of the His-tagged recombinant proteins expressed in transformed bacteria (left). A prominent 25-kDa His-tagged recombinant protein (arrowhead) in the extract supernatant (pre) from IPTG-induced bacteria is effectively removed by Ni-NTA affinity chromatography (post). The bound protein is eluted from the affinity matrix by imidazole buffer (Elute). Western analysis shows that the antibody raised against the recombinant protein recognizes a single 24-kDa protein that is present in wild type but absent in *pf*14 (right). The Ponceau-stained blot demonstrates equal protein loading. (D) Sequencing of PCR product shows that a G-to-A mutation (boxed letter) in the 5′ UTR of the RSP11 gene in *pf*25A, resulting in an upstream ATG and an open reading frame for a distinct polypeptide of 72-amino acid residues (bold). The original first methionine is underlined.

ticle (Figure 3C, arrowheads). Thus, these results indicated that the new spoke RIIa protein and AKAP are stably located toward the base of spokestalk, near outer doublet and dynein motors.

Deficiency in RSP11 Does Not Affect General Assembly and Stability of pf25 Radial Spokes

To further examine *pf*25 radial spokes, silver-stained 2-D gels of wild-type and *pf*25 axonemes were compared (Figure 4A). The 10 major spoke proteins that can be unequivocally identified at the acidic end of 2-D gel (labeled by numbers in Figure 4A) were normal in *pf*25 except for RSP11, consistent with a previous description (Huang *et al*., 1981). To test the stability, the spokes were extracted with 0.6 M KI and fractionated by sucrose gradient sedimentation. Extracted *pf*25 radial spokes were shown by RSP3 Western to sediment as 20S wild-type spoke particles (arrowhead), whereas the *pf*24 spokes unstable at the head end are smaller (Figure 4B). 2-D gel analyses did not reveal significant difference in composition between the 20S spoke particles from *pf*25 and wild-type except for RSP11 as well (our unpublished data).

Direct Association of RSP11 and RSP3

To test direct binding, RSP11 overlays were carried out. Axonemal samples separated by SDS-PAGE were blotted to nitrocellulose membrane. Part of the blot was overlaid with recombinant RSP11–6 His, and binding was revealed by anti-His and secondary antibody (Figure 4A, left). The rest of the membrane was processed for RSP3 immunoblot (Figure 5A, right). As for PKA RII (Gaillard *et al*., 2001), recombinant RSP11 binds an ~83-kDa band that is present in the axonemes of various strains except *pf*14 (Figure 5A, left, arrowhead) and comigrates with RSP3 revealed by Western blots (Figure 5A, right).

To simulate the in vivo environment, a pull-down assay was performed. The expression constructs for RSP11–6His and GST-RSP3 were cotransformed into bacteria. Bacterial supernatant was subjected to Ni-NTA affinity purification (Figure 5B, left). The control group was transformed with the GST-RSP3 construct only (Figure 5B, right). The recombinant GST-RSP3 and RSP11–6His, revealed by Coomassie protein gel, were soluble in the extract, effectively depleted in the flow through of the Ni-NTA matrix, and copurified in the matrix fraction (Figure 5B, left, compare Pre, Post, and Ni-NTA). In contrast, there was no obvious binding of GST-RSP3 to Ni-NTA in the control lacking RSP11–6His (Figure 4B, right). GST alone also did not copurify with RSP11–6 His (our unpublished data). Chemical cross-linking that demonstrated direct interaction of several axonemal proteins (Yang *et al*., 2001, 2005) cannot definitively reveal the interaction of RSP11 and RSP3, possibly because of the hydrophobic interaction between RIIa domain and the amphipathic helix.

Unusual Motility Phenotype of RSP11 Mutant pf25

To elucidate the function of RSP11, we investigated the motility phenotype of *pf*25 that was described as "swim

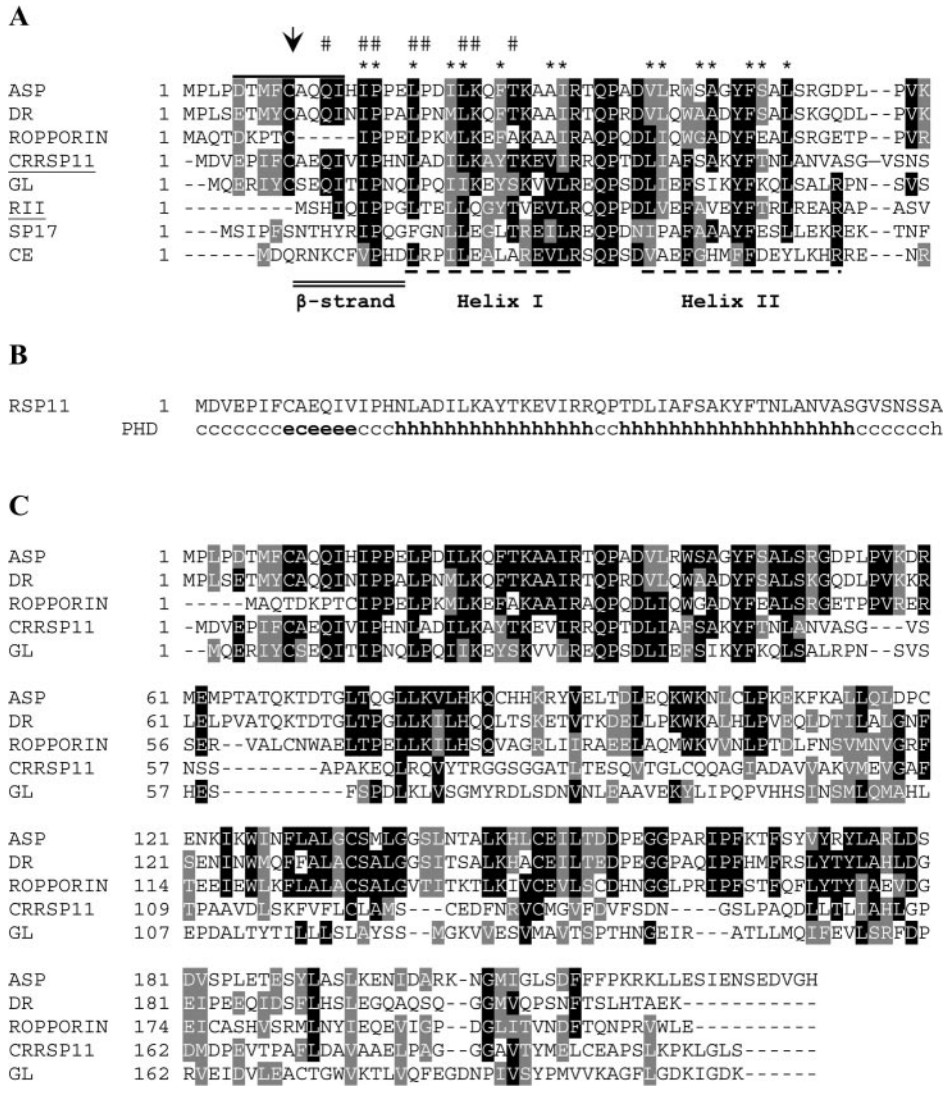

Figure 2. Sequence analysis of RSP11 predicted protein sequence. (A) Sequence alignment of the RIIa domain in RSP11, mouse RII (underline), and several representative ~20-kDa homologous proteins revealed by Blastp search. The β-strand, two helices and the residues binding the amphipathic helix of AKAP (asterisks) are based on the NMR study of RII (Banky *et al*., 2000; Newlon *et al*., 2001). Additional homology is present at the extreme N terminus in four of these proteins (arrow). Listed proteins are human ASP (AKAP-associated sperm protein; NP_114122), human ropporin (AAG27712), human SP17 (Q15506), GL (EAA39937; *Giardia lamblia*), DR (AAH81402; zebra fish), and CE (AAA83605; *C. elegans*). (B) PHD analysis reveals that as RII, the N terminus of RSP11 also consists of β-strand preceding the two helices (bold letters). (C) The C termini of RIIa proteins diverge significantly. ASP, ropporin, and similar proteins from other vertebrates such as zebra fish (DR) are homologous throughout the entire protein, whereas the C termini of RSP11 and the *Giardia* protein differ from each other and the rest significantly.

actively, but in an abnormal manner" (Huang *et al*., 1981). Surprisingly, we initially could not distinguish wild-type and *pf*25 cells taken from 8-l culture meant for axonemal preparation (Figure 3B) under light microscopy. However, careful observation revealed that a few cells have paralyzed or twitching flagella. The numbers of paralyzed cells varied among different preparations. To determine whether the mixed motility is limited to the particular allele or caused by spontaneous mutation, we examined the three available alleles, *pf*25A, D, and F, that were also generated by chemical mutagens and that had been backcrossed to wild type previously (Huang *et al*., 1981). Consistently, all of the *pf*25 alleles lacked RSP11 (Figure 6A) and displayed mixed motility. Furthermore, we backcrossed *pf*25(−) again with wild-type strain cc125(+). Among the 11 sets of tetrads, as illustrated in the representative Westerns, the ratio of *pf*25 and wild-type motility phenotype was 1:1, and the former always cosegregated with RSP11 deficiency, whereas RSP16 was normal (Figure 6B). Thus, the analyses of four independent alleles and backcrossed progeny strongly indicate the mixed flagellar motility of *pf*25 is because of defective RSP11 gene.

To determine when the mixed motility develops, *pf*25 cells were observed several times daily after the initial inoculation. *Pf*25 and wild-type cells generated full-length flagella within 2 h once cells maintained on agar plates were resuspended in liquid media. Interestingly, the flagella of freshly resuspended *pf*25 cells predominantly were paralyzed or twitching like other radial spoke mutants. Occasionally, one or two cells were found tumbling or actively swimming. The second day, most cells had twitching flagella. Some even could circle or rotate along the longer axis of the cell body. More cells were able to swim in the signature helical pattern as wild type until the fourth day with cell density of $\sim 2 \times 10^6$ cells/ml. The variation of flagellar motility is illustrated by the three panels of images taken within 1.1 s (Figure 7, live image is shown by videomicroscopy as Supplemental Material). The twitching flagella and the swimming cells are highlighted with black and white arrowheads, respectively. The trend of improvement is illustrated by increased percentage of swimmers and reduced percentage of cells with twitching flagella over the 4-d period (Figure 8A). Similar results were obtained from 16 independent cultures derived from single colonies or by using the better buffered TAP media (Tris-acetate-phosphate buffer listed in Harris, 1988) (our unpublished data). The changes were not as obvious in the same day as they were overnight.

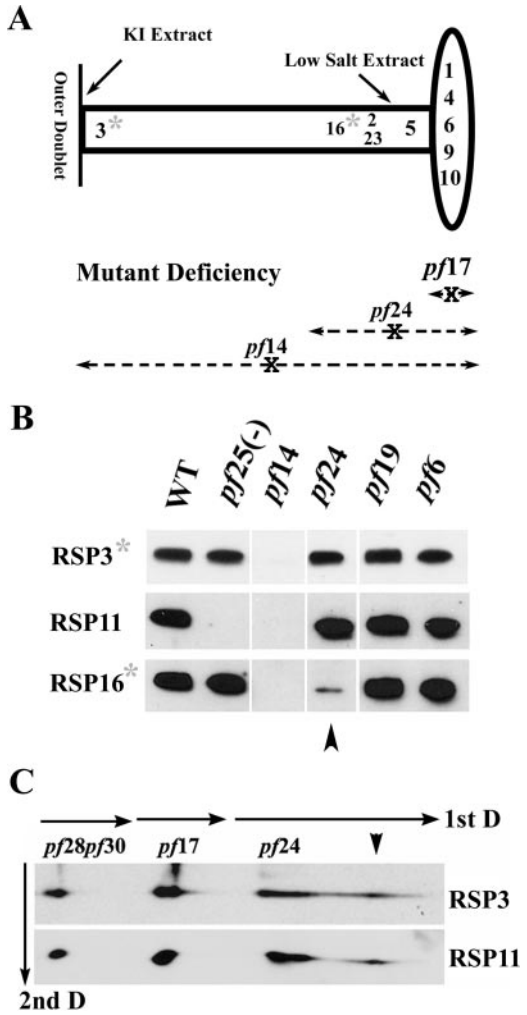

Figure 3. RSP11 is a RIIa protein colocalized with RSP3 toward the base of radial spokes. (A) Schematic (after Curry and Rosenbaum, 1993) highlighting topography of radial spokes and deficiency in spoke mutants (dashed line) *pf*14, *pf*17, and *pf*24. RSP3 and RSP16 (gray asterisks) are located toward the opposite ends of the stalk region. (B) Western analysis shows that antirecombinant RIIa protein recognizes a 24-kDa protein in the axonemes from various *Chlamydomonas* strains except the spokeless mutant *pf*14 and RSP11 mutant *pf*25. Westerns of RSP3 and RSP16 (gray asterisks) verify that RSP16 is diminished in *pf*24 (arrowhead), a mutant defective in the head end of spokes, whereas RSP3 and RSP11 are normal. (C) RSP11 and RSP3 colocalized in the defective spoke particles (arrow) extracted from *pf*24. Sucrose gradient peak fractions of wild-type spoke from dynein mutants, spokestalk from headless *pf*17, and spoke particles from *pf*24 (Yang *et al*., 2005) are first fractionated in blue native gel, followed by SDS-PAGE, and Westerns. In contrast to wild-type spoke or *pf*17 spokestalk, the *pf*24 spokes were separated as several distinct particles. Nonetheless, RSP11 always colocalized with RSP3, including the smallest particle (arrowhead). Arrow indicated the direction of current.

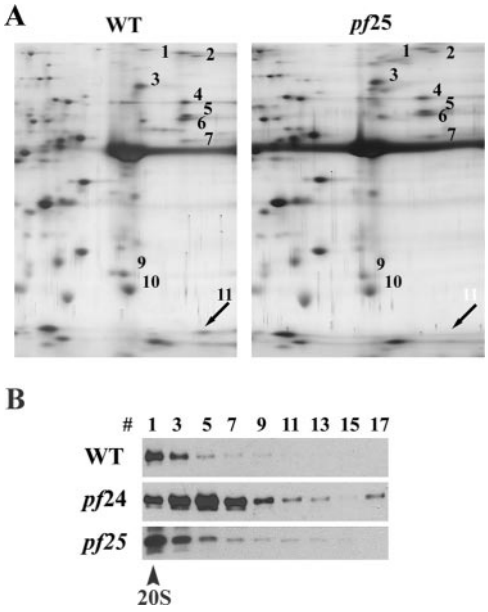

Figure 4. No obvious assembly defect in *pf*25 radial spokes. (A) The radial spoke proteins (numbered) that are easily identified at the acidic half of 2-D silver gel seem normal in *pf*25 except that RSP11 is absent (arrow). Acid end is at the right side. (B) Western blot of sucrose gradient of radial spoke extract from WT, *pf*24, and *pf*25 cells showed that *pf*25 radial spokes, revealed by RSP3, sediments like the 20S WT radial spoke (arrowhead), whereas *pf*24 spokes are significantly smaller because of the defect at the head end of radial spokes.

To test whether the acquired motility was sustained, two 4-d-old cultures were continued. Surprisingly, percentage of swimmers was reduced dramatically as the culture reached stationary phase the next day, even though the flagellar length was similar (Figure 8B, white bar). On the contrary, the control *pf*25 cells, transferred into equal amount of fresh media daily, retained the motility better (black bar). Importantly, wild-type (WT) cells cultured side by side under the same condition swim constantly (our unpublished data).

To test that medium condition determined the overall motility, a 4-d-old 300-ml culture was divided into three equal aliquots. One pellet was resuspended back into the medium from which the cells were harvested, whereas the other two pellets were transferred to fresh medium or spent medium in which paralyzed cells from the prolonged culture had been removed. Again, 1 d later, a higher percentage of cells in the fresh medium were swimming, whereas most cells in the exhausted medium were paralyzed (Figure 8C).

To investigate another allele independently and to test whether *pf*25 cells swim slower than wild type, the swimming velocity of *pf*25A was measured. Like *pf*25(−), none of *pf*25A cells in the first day are swimming in the random sampling, but the number of swimmers gradually increased. For those swimming with a helical path, the averaged velocity improved over the next 3 d but slowed down dramatically on the fifth day (Figure 9, hatched bar), consistent to the changes in percentages (Figure 8). In contrast, wild-type cells grown in same condition and similar density always swam, and the velocity did not fluctuate so dramatically (Figure 9, stippled bar). Notably, the velocity of *pf*25 was equivalent to wild-type on the fourth day (Figure 9, compare stippled and solid bars), suggesting that the deficiency in *pf*25 does not significantly compromise mechanical property of *pf*25 axonemes. Similarly, swimmers in day 2 culture can be stopped by 5% viscous ProtoSlow, whereas 10% ProtoSlow is required to stop *pf*25 swimmers on day 3 and slow down *pf*25 swimmers and wild type equally on day 4 (our unpublished data). Together, these results reveal that the motility of *pf*25 in terms of percentages of swimmers and

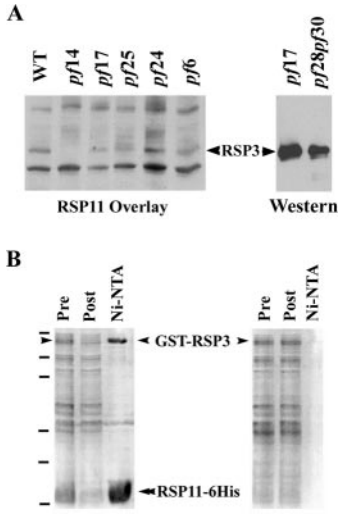

Figure 5. RSP11 associates with RSP3, the spoke AKAP. (A) An overlay assay using RSP11-6 His as a probe shows that RSP11 binds an 83-kDa protein in axonemes prepared from various strains except the RSP3 mutant, *pf*14 (left). The probe is revealed by anti-His and anti-mouse antibodies. The 83-kDa protein comigrates with RSP3 is revealed by Western blot of axoneme samples (right). (B) Pull-down assay. GST-RSP3 (arrowheads) and RSP11–6 His (double arrowheads) are present in the supernatant (pre) of bacteria transformed with both constructs (left). Both proteins are effectively depleted in the flow through (post) after Ni-NTA chromatography. Pull down of the His-tagged protein results in the copurification of GST-RSP3. In contrast, no specific binding to Ni-NTA is detectable in the control group that expresses GST-RSP3 only (right).

swimming velocity is overtly sensitive to media conditions, whereas the output potential remains intact.

In light of the well recognized effect of medium on gametic differentiation (Martin and Goodenough, 1975), we tested the hypothesis that the shift of *pf*25 motility is related

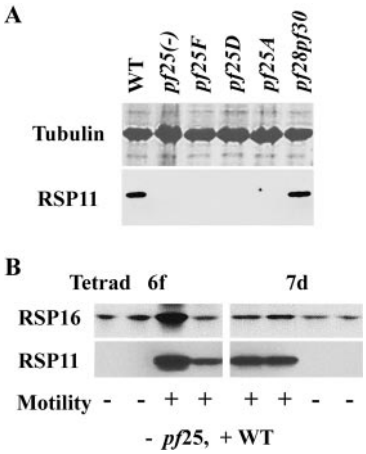

Figure 6. Pf25 motility defect is tightly linked to the absence of RSP11. (A) Western analysis of axonemes reveals that RSP11 is absent in all of the *pf*25 alleles but normal in wild type and dynein mutant *pf*28*pf*30. (B) Western blot and motility study of tetrad meiotic progeny show a 1:1 ratio of motility phenotypes. The progeny displaying *pf*25 motility phenotypes always lack RSP11. RSP16 Western is a control. Two representatives of the 11 complete tetrad groups are shown.

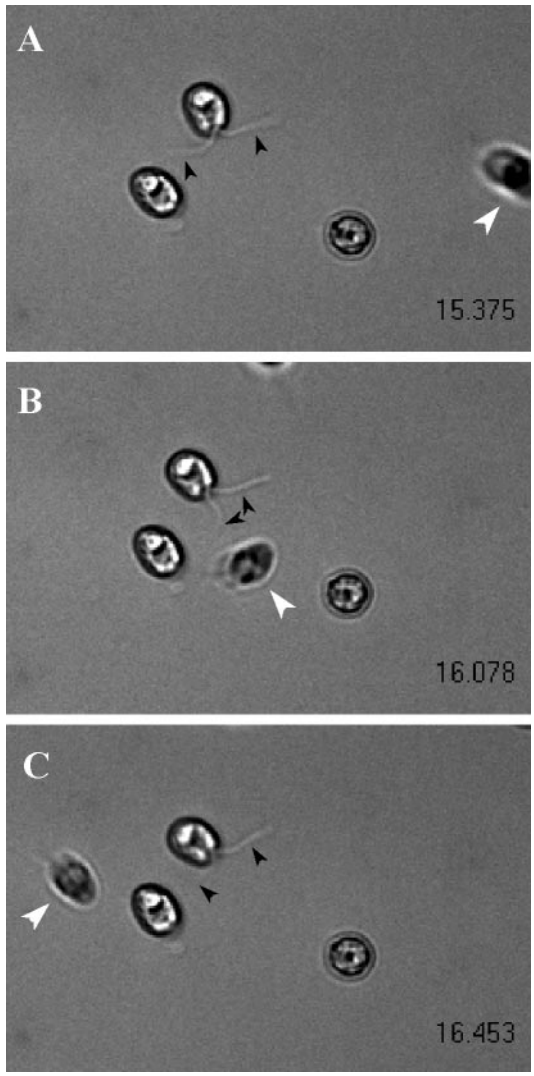

Figure 7. Pf25 cells in the same culture demonstrate different motility level. Three panels of bright-field microscopy taken at the time indicated in seconds at bottom right corner show that one cell is swimming (clear arrowhead), whereas the other has twitching flagella (black arrowheads). The flagella of the other two cells stuck to glass are out of focus. Motion picture that includes the three panels is shown in the video in the Supplemental Material.

to the gametic differentiation induced by nitrogen depletion. The *pf*25(−) cells cultured on TAP plate for a week successfully differentiated into gametes that mate with wild-type cc620 (−) once resuspended in nitrogen-depleted medium (Saito *et al*., 1993). However, no obvious difference in motility was observed between the gametic cells and vegetative control cells that were resuspended in nitrogen-containing medium in a similar manner and could not mate (our unpublished data). Most cells in both groups had flaccid or twitching flagella, whereas a small number of cells could swim actively. This result indicates that "the active swimming in an abnormal manner" of *pf*25 cells that are prepared as gametic cells freshly resuspended in nitrogen-free medium (Huang *et al*., 1981) resembles the motility of vegetative cells in nitrogen-containing medium in the first day or two, as shown in this study. Together, the negative results indicate that the medium-dependent shift of motility is not simply because of gametic differentiation.

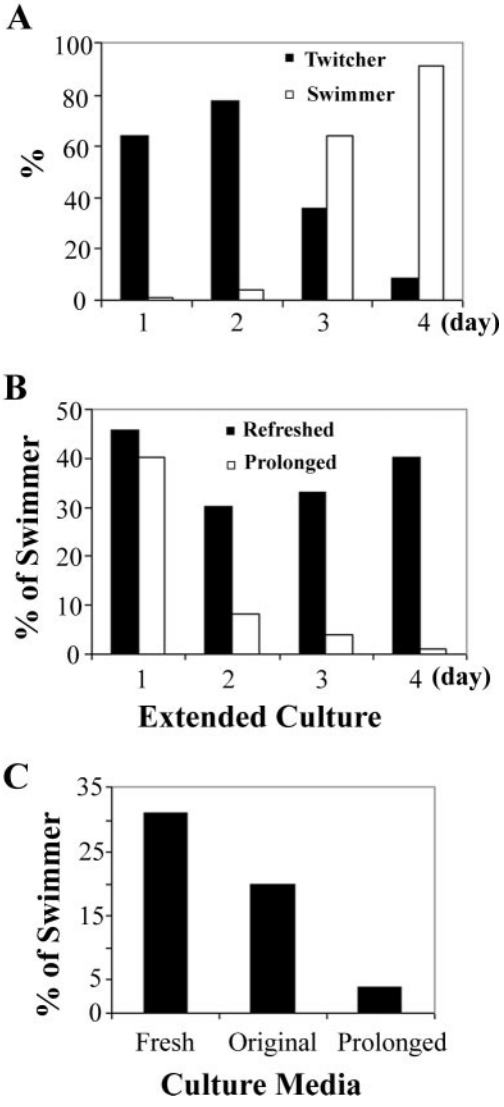

Figure 8. Flagellar motility of *pf*25 cells is reversibly affected by culture media. (A) Cultures of *pf*25(−) are assessed for four consecutive days by bright-field light microscopy after inoculation. On the first day, few cells swim, whereas most are twitching (black bar). The rest with immotile flagella are not included. As culture progresses, more cells are able to swim (open bar), whereas the cells with twitching flagella reduced until the fourth day. The percentage is determined based on the observation of 500 counted cells at least. (B) Most of the *pf*25 cells are paralyzed in the confluent culture extended beyond the initial 4-d period (white bar). However, daily transfer of harvested cells into fresh medium (black bar) prevents severe decline in motility. (C) Freshness of media affects percentage of swimmers in *pf*25 culture. The motility is assessed one day after the cell aliquots from a 4-d-old liquid culture were resuspended into 300-ml fresh medium, saved 4-d-old medium or a 6-d-old exhausted medium that paralyzed cells have been removed.

To test whether the altered motility is because of the restored proteins or phosphorylation, axonemes were prepared from paralyzed or twitching cells freshly resuspended from agar plates or from a 4-d-old liquid culture containing >70% swimmers. Compared with wild-type axonemes, RSP11 is absent and RSP8 is reduced in *pf*25 as stated by Huang *et al*. (1981), whereas the amount of RSP16 is normal (Figure 10A, compare first two lanes). However, there was

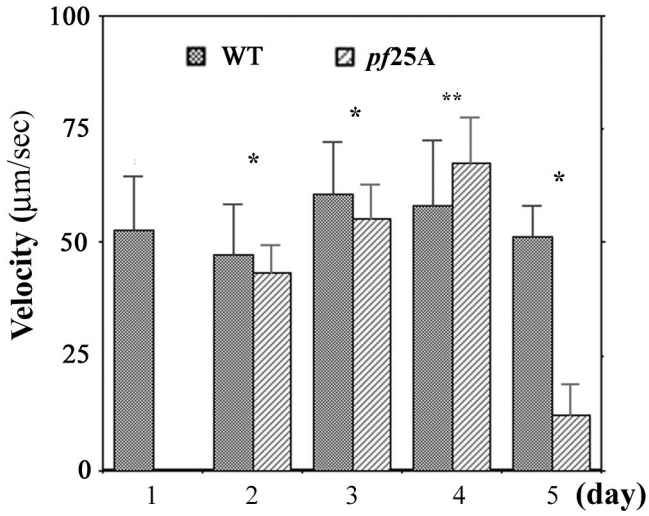

Figure 9. Pf25 cells can swim as fast as wild-type cells. The wild-type and *pf*25A cells are recorded for five sequential days. No swimming *pf*25 cells are found during random sampling in the first day. The velocity of swimming *pf*25 cells improves over the first 4 d and then declines in the fifth day (hatched bar). In contrast, the swimming velocity of wild-type cells during the same period fluctuates less significantly (stippled bar). The swimming velocity of *pf*25 cells is slower than WT in day 2, 3, and 5 (single asterisks, $p < 0.023$, Student's t test). Importantly, no significant difference between *pf*25 cells at the peak condition and wild-type cells (double asterisks, $p > 0.05$) on the fourth day. The individual cells swimming in a helical path are tracked (n = 25–30 for each data point) and velocity determined by MetaMorph software.

no significant difference between the two groups of *pf*25 cells (Figure 10A, compare the second and third lanes.). Phosphorylation cannot account for the *pf*25 motility phenotype either (Figure 10B; Huang *et al*., 1981). Two major phosphorylated proteins, RSP2 and 3, were predominantly phosphorylated in wild type, paralyzed *pf*25, and swimming *pf*25. In contrast, more dephosphorylated RSP3 (arrowhead) was

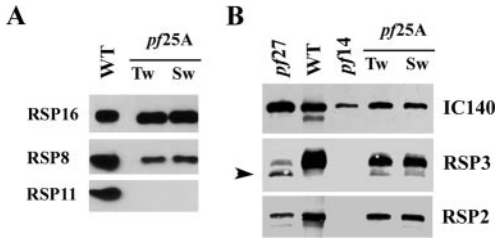

Figure 10. The switches of *pf*25 motility are not related to changes in defective proteins or phosphorylation state of radial spokes. Axonemes prepared from control strains and freshly resuspended *pf*25 cells with twitching flagella (tw) and *pf*25 liquid culture with >70% swimmers (sw) are evaluated by Western blots. (A) Neither RSP11 nor RSP8 is restored in the swimming *pf*25A cells. Compared with wild type, RSP8 and RSP11 in the axonemes of *pf*25A cells are reduced and undetectable, respectively. However, there is no significant difference between twitching and swimming *pf*25 cells. RSP16 western is a control. (B) Two major phosphorylated spoke proteins, RSP2 and 3 in the two *pf*25 samples are not significantly different from those in wild type. In contrast, RSP3 is more dephosphorylated (arrowhead), and both RSP2 and RSP3 are reduced in *pf*27 as shown previously (Huang *et al*., 1981). Western blot of dynein IC140 shows the protein loading level.

present in *pf*27 that has paralyzed flagella and defective phosphorylation and assembly of radial spokes (Huang *et al*., 1981).

DISCUSSION

This study demonstrates that RSP11 gene encodes a new RIIa protein that associates with RSP3 at the basal end of spokestalk. These findings strongly support previous identification of RSP3 as an AKAP (Gaillard *et al*., 2001) albeit the RIIa protein is not RII of PKA. Intriguingly, RSP11 mutant displays dramatic switches of motility phenotypes as a function of medium conditions, indicating that the spoke RIIa protein is essential for normal flagellar beating and possibly for regulation. These findings shed new light on the complexity of the regulatory mechanisms mediated by radial spokes.

RSP11, RSP3, and the Regulatory Mechanism of Radial Spokes

RSP11 is unequivocally an RIIa protein and *pf*25 is an RSP11 mutant based on the following evidence. 1) The sequence founded on mass spectrometry polypeptides from spot-purified RSP11 of isolated radial spokes predicts an RIIa protein consistent to the size and pI of RSP11. 2) Mapping with 3′ UTR sequence indicates that RSP11 gene is located distal to molecular markers GP52 and CNA26 in the linkage group X, consistent with the predicted location of *PF*25. 3) RSP11 gene rescues *pf*25. 4) Antibodies raised against the recombinant RIIa protein recognize a 24-kDa protein that is present in all of the strains tested except *pf*14 and *pf*25. 5) Sequencing of genomic DNA reveals a point mutation at 5′ UTR of *pf*25A. 6) Dikaryon rescue of *pf*25 shows that *pf*25 cells synthesize all of the spoke proteins except RSP11 (Huang *et al*., 1981). As predicted, RSP11 binds to spoke AKAP. Mutant analyses and biochemical extraction further indicates that both proteins colocalize toward the base of spokestalk in axonemes (Figures 3 and 5).

The finding of non-PKA RIIa protein in radial spokes is unexpected. Diverse evidence suggests that radial spokes control dynein activity through phosphoenzymes, including PKA (reviewed by Porter and Sale, 2000), and RSP3 binds PKA RII in vitro (Gaillard *et al*., 2001). Rather, this study demonstrated that RSP3 binds RSP11, a non-PKA RIIa protein and that phosphorylation seems unrelated to *pf*25 abnormally regulated motility, suggesting that RSP3/RSP11 mediate a non-PKA regulatory mechanism. One interpretation is that RSP3 does not bind PKA or mediate cAMP-dependent regulation and that PKA pathway is mediated by other mechanisms.

However, equally possible is that in addition to RSP11, RSP3 may bind RII and/or other RIIa proteins. Dual-specific AKAPs interact with multiple RIIa proteins. Emerging evidence indicates that the association could be reversible and modulated. For example, fibrous sheath AKAP3 binds RI, RII, CABYR, SP17, ASP, and ropporin (Carr *et al*., 2001; Naaby-Hansen *et al*., 2002; Lea *et al*., 2004; reviewed by Eddy *et al*., 2003), and phosphorylation increases its binding to RIIβ and PKA recruitment (Luconi *et al*., 2004). In addition, the RIIa domains from various proteins are not equivalent in AKAP binding. The regions N terminal to RIIa domains in RI and RII assume distinct secondary structures (Banky *et al*., 2000) that may account for the different affinity and binding sites for RI and RII on dual-specific AKAPs (Huang *et al*., 1997; Burns-Hamuro *et al*., 2004; Salvador *et al*., 2004). The RIIa domains of RSP11, ASP, and *Giardia* protein but not RII share stronger similarity (Figure 2), suggesting that RSP11 may not share the mapped binding sites for RII (Gaillard *et al*., 2001). It will be interesting to test whether RSP3 is a dual-specific AKAP as well. Both hypotheses support the central concept that RSP3, as a spoke AKAP, anchors regulatory pathways to the spoke complex and near dynein motors (Gaillard *et al*., 2001).

The Molecular Interaction of RSP11

*Pf*25 is the only known spoke mutant that does not have morphological defect and is capable of swimming (Huang *et al*., 1981). The limited defect in RSP11 and RSP8 indicates that these two constitutive components are not essential for the assembly and the core structure of the T-shaped complex that consists of ~23 proteins (Yang *et al*., 2001). Rather, they may be peripheral functional components. The indirect overlay and effective pull-down of RSP3 by RSP11 affinity (Figure 5) suggest that the affinity is likely equivalent to RII/AKAP affinity that suffices RII overlays and the purification of an oligomeric complex (Lohmann *et al*., 1984; Bregman *et al*., 1989). However, similar to the challenge of studying fibrous sheath AKAPs, the extreme stability of cytoskeletal structure and the central role of RSP3 in the assembly of radial spokes prevent further purification of RSP11/RSP3 complex. Nonetheless, the colocalization of both proteins in the basal part of the spokestalk from *pf*24 mutants (Figure 3) is equivalent to or exceeds the current resolution of immunoprecipitation or immunolocalization of RIIa proteins and AKAPs in flagellar compartments (Carr *et al*., 2001; Lea *et al*., 2004; Rawe *et al*., 2004).

Despite the high affinity, RSP3 may not be the sole protein that harnesses RSP11 to the structural complex. Instead, the reduction of RSP8 in *pf*25 (Figure 10; Huang *et al*., 1981) suggests that RSP8 interacts with RSP11, most likely its C terminus, as well. The defective interactions among the three proteins likely account for the abnormally regulated motility of *pf*25.

To Beat or Not to Beat of Pf25 Flagella

The *pf*25 phenotype reveals the functional significance of RSP11 and possibly a novel regulatory mechanism that is not obvious in wild-type *Chlamydomonas*. The motility of *pf*25 is unique in two aspects. 1) *Pf*25 cells display a spectrum of motility in the same culture. The paralysis state resembles the other spoke mutants that have flaccid or twitching flagella correlated with gross structural defects. In contrast, *pf*25 cells originated from the same colony in a few days can swim like wild-type cells and then become paralyzed again. 2) The dramatic swing in overall motility level occurs during regular culture period, depending on how fresh (or how old) the medium is.

To our knowledge, until this study, the flagellar motility of wild-type and mutant strains during the culture period had not changed significantly enough to inspire investigation. Wild-type *Chlamydomonas* cells seem to swim constantly in a smooth helical path (Harris, 1988) without obvious changes in motility (Figure 9) unless physical stimuli transiently alter flagellar beating (see below). Most of the motility mutants are generated by mutagens, X-rays, or insertional mutagenesis and have stable single phenotypes as anticipated. Mutations in motors or other axonemal complexes are manifested as reduced swimming velocity, different beating patterns, or swimming path or paralysis (Huang *et al*., 1981; Brokaw and Kamiya, 1987; Perrone *et al*., 2000). Mutants screened for defective signaling pathways (Pazour *et al*., 1995) fail to respond to stimuli without affect normal flagellar beating. Regardless of the severities of motility

defects or nature of mutation, no reports have indicated shift of mixed motility as *pf*25.

It is not clear what causes the reversible switches. The switches seem different from the changes induced by second messengers. Light elicits phototaxis or photoshock is mediated by transient fluctuation of intraflagellar Ca^{2+}, maybe partly through radial spokes (Schmidt and Eckert, 1976; Bessen *et al*., 1980; Brokaw *et al*., 1982; Kamiya and Witman, 1984). Reagents that increase cAMP concentration or cAMP analogues inhibit *Chlamydomonas* flagellar motility, although the physiological relevance is not clear (Rubin and Filner, 1973; Hasegawa *et al*., 1987). Notably, these reactions occur within milliseconds to minutes, whereas effects of medium on *pf*25 cells are more noticeable overnight and are observed in portions of population instead of every cell. Furthermore, twitching flagella or tumbling cells seem to be a transitional stage between paralysis and wild-type swimming. Therefore, the regulatory mechanism that becomes obvious in the absence of RSP11 differs from the on-off responses induced by cAMP and calcium. Rather, reactions within cell body may be involved. Consistent to this interpretation, attempts to rescue the paralyzed *pf*25 cells by changing concentration of the second messengers and broad-spectrum inhibitors to kinase activated by second messengers have not succeeded. Neither can adjusting pH nor using the stronger buffered TAP medium change *pf*25 motility phenotypes (our unpublished data).

Additional mutation or selection of subpopulation of cells is ruled out because of the reversibility, cultures from single colonies and tight correlation of genetic and motility phenotypes among backcrossed progeny (Figures 6–9). Normal ultrastructure and composition, stability of spoke complex (Huang *et al*., 1981; Figure 4 and 5), and the wild-type like velocity and smooth helical path strongly suggest that the mechanism of *pf*25 radial spokes and axonemes is largely intact. The simplest explanation is that the *pf*25 is as capable as wild type in flagellar beating, but an abnormal regulatory mechanism shuts down the beating in the unfavorable conditions. Paradoxically, the gain of sensitivity is because of loss of spoke RIIa protein. Conceivably, the heightened sensitivity could be because of a misplaced regulatory protein that normally associates with RSP11 or RSP8. Or, the regulator normally suppressed by RSP11 becomes active in *pf*25 flagella. Alternatively, other proteins that normally do not associate with RSP3 become accessible to RSP11 binding site when RSP11 is absent, albeit with lower affinity. Regardless the detail mechanism, the reversible nature of *pf*25 phenotype supports the postulated chemical signal transduction mediated by radial spokes.

Non-PKA RIIa Proteins

Previous studies have shown that non-PKA RIIa proteins are abundant in sperm and hence suggest that they are unique to male germ cells (Carr *et al*., 2001). RSP11/RSP3 complex in the typical feature of 9 + 2 cilia and flagella argues otherwise. Although RSP11 orthologues cannot be identified definitively, EST sequences homologous to RSP3 are present in different tissues in mammals and other organisms, including vertebrates, insects, *Ciona* (Gaillard *et al*., 2001; Koukoulas *et al*., 2004), and *Giardia*. The extensive homology suggests that RSP3 is conserved to target the radial spoke (Huang *et al*., 1981; Diener *et al*., 1993) as well as RIIa proteins. Thus, RIIa/RSP3 is likely a common feature of 9 + 2 cilia and flagella. In line with this prediction is the detection of one RIIa protein, SP17, in various tissues, notably in cilia as well (Frayne and Hall, 2002; Grizzi *et al*., 2004).

Despite the divergence, the C termini of RIIa proteins (Figure 2C) may confer special regulatory mechanism tailored for individual cell types. For example, CABYR (fibrousheathin II; AAC35373) may mediate calcium-dependent regulatory pathways via their EF-hand for calcium binding (Naaby-Hansen *et al*., 2002), whereas SP17 (Q15506) uses its calcium/calmodulin-binding IQ motifs (Lea *et al*., 2004). The C-terminal peptide of ropporin lacks recognizable modules but still associates with rhophilin, a Rho-binding protein (Nakamura *et al*., 1999; Fujita *et al*., 2000). Further study on the C terminus of RSP11 likely will reveal the new regulatory mechanism of radial spokes and nonconventional AKAPs.

The suppressor mutants inspired the hypothesis that the radial spoke is part of a system that controls flagellar motility (Huang *et al*., 1982). This study provides the in vivo evidence supporting the hypothesis and reveals a spoke non-PKA RIIa protein possibly mediating a new regulatory mechanism in diverse cilia and flagella. The evidence in green algae and the broad presence of non-PKA RIIa proteins sharing the targeting domain of PKA in eukaryotes indicate that they are not evolutionary mishaps or specially evolved for male germ cells. Rather, they should be considered as part of the growing repertoire of the diverse regulatory pathways that AKAPs may integrate.

ACKNOWLEDGMENTS

We are grateful to Dr. U. W. Goodenough (Washington University, St. Louis, MO) for advice on gametic differentiation; Nancy Hass and Dr. C. D. Silflow (University of Minnesota, St. Paul, MN) for mapping RSP11 gene; and Dr. L. W. Tam for advice on transformation and tetrad dissection (University of Minnesota). We also thank Dr. Dennis Diener and J. L. Rosenbaum (Yale University, New Haven, CT) for anti-RSP3 and the expression construct of GST-RSP3. This study is supported by National Institutes of Health Grant GM-068101.

REFERENCES

Amieux, P. S., and McKnight, G. S. (2002). The essential role of RI alpha in the maintenance of regulated PKA activity. Ann. N.Y. Acad. Sci. *968*, 75–95.

Banky, P., Newlon, M. G., Roy, M., Garrod, S., Taylor, S. S., and Jennings, P. A. (2000). Isoform-specific differences between the type Ialpha and IIalpha cyclic AMP-dependent protein kinase anchoring domains revealed by solution NMR. J. Biol. Chem. *275*, 35146–35152.

Bessen, M., Fay, R. B., and Witman, G. B. (1980). Calcium control of waveform in isolated flagellar axonemes of *Chlamydomonas*. J. Cell Biol. *86*, 446–455.

Bregman, D. B., Bhattacharyya, N., and Rubin, C. S. (1989). High affinity binding protein for the regulatory subunit of cAMP-dependent protein kinase II-B. Cloning, characterization, and expression of DNAs for rat brain P150. J. Biol. Chem. *264*, 4648–4656.

Brokaw, C. J., and Kamiya, R. (1987). Bending patterns of *Chlamydomonas* flagella: IV. Mutants with defects in inner and outer dynein arms indicate differences in dynein arm function. Cell Motil. Cytoskeleton. *8*, 68–75.

Brokaw, C. J., Luck, D. J., and Huang, B. (1982). Analysis of the movement of *Chlamydomonas* flagella: the function of the radial-spoke system is revealed by comparison of wild-type and mutant flagella. J. Cell Biol. *92*, 722–732.

Burns-Hamuro, L. L., Barraclough, D. M., and Taylor, S. S. (2004). Identification and functional analysis of dual-specific A kinase-anchoring protein-2. Methods Enzymol. *390*, 354–374.

Carr, D. W., Fujita, A., Stentz, C. L., Liberty, G. A., Olson, G. E., and Narumiya, S. (2001). Identification of sperm-specific proteins that interact with A-kinase anchoring proteins in a manner similar to the type II regulatory subunit of PKA. J. Biol. Chem. *276*, 17332–17338.

Curry, A. M., and Rosenbaum, J. L. (1993). Flagellar radial spoke: a model molecular genetic system for studying organelle assembly. Cell Motil. Cytoskeleton *24*, 224–232.

Dell'Acqua, M. L., Dodge, K. L., Tavalin, S. J., and Scott, J. D. (2002). Mapping the protein phosphatase-2B anchoring site on AKAP79. Binding and inhibition of phosphatase activity are mediated by residues 315–360. J. Biol. Chem. *277*, 48796–47802.

Diener, D. R., Ang, L. H., and Rosenbaum, J. L. (1993). Assembly of flagellar radial spoke proteins in *Chlamydomonas*: identification of the axoneme binding domain of radial spoke protein 3. J. Cell Biol. *123*, 183–190.

Eddy, E. M., Toshimori, K., and O'Brien, D. A. (2003). Fibrous sheath of mammalian spermatozoa. Microsc. Res. Tech. *61*, 103–115.

Frayne, J., and Hall, L. (2002). A re-evaluation of sperm protein 17 (Sp17) indicates a regulatory role in an A-kinase anchoring protein complex, rather than a unique role in sperm-zona pellucida binding. Reproduction *124*, 767–774.

Fujita, A., Nakamura, K., Kato, T., Watanabe, N., Ishizaki, T., Kimura, K., Mizoguchi, A., and Narumiya, S. (2000). Ropporin, a sperm-specific binding protein of rhophilin that is localized in the fibrous sheath of sperm flagella. J. Cell Sci. *113*, 103–112.

Gaillard, A. R., Diener, D. R., Rosenbaum, J. L., and Sale, W. S. (2001). Flagellar radial spoke protein 3 is an A-kinase anchoring protein (AKAP). J. Cell Biol. *153*, 443–448.

Martin, N. C., and Goodenough, U. W. (1975). Gametic differentiation in *Chlamydomonas reinhardtii*. I. Production of gametes and their fine structure. J. Cell Biol. *67*, 587–605.

Grizzi, F., *et al*. (2004). Sperm protein 17 is expressed in human somatic ciliated epithelia. J. Histochem. Cytochem. *52*, 549–554.

Habermacher, G., and Sale, W. S. (1997). Regulation of flagellar dynein by phosphorylation of a 138-kD inner arm dynein intermediate chain. J. Cell Biol. *136*, 167–176.

Harris, E. H. (1988). The *Chlamydomonas* Sourcebook, San Diego: Academic Press.

Hasegawa, E., Hayashi, H., Asakura, S., and Kamiya, R. (1987). Stimulation of *in vitro* motility of *Chlamydomonas* axonemes by inhibition of cAMP-dependent phosphorylation. Cell Motil. Cytoskeleton *8*, 302–311.

Hendrickson, T. W., Perrone, C. A., Griffin, P., Wuichet, K., Mueller, J., Yang, P., Porter, M. E., and Sale, W. S. (2004). IC138 is a WD-repeat dynein intermediate chain required for light chain assembly and regulation of flagellar bending. Mol. Biol. Cell *15*, 5431–5442.

Howard, D. R., Habermacher, G., Glass, D. B., Smith, E. F., and Sale, W. S. (1994). Regulation of *Chlamydomonas* flagellar dynein by an axonemal protein kinase. J. Cell Biol. *127*, 1683–1692.

Huang, B., Piperno, G., Ramanis, Z., and Luck, D.J.L. (1981). Radial spokes of *Chlamydomonas* flagella: genetic analysis of assembly and function. J. Cell Biol. *88*, 80–88.

Huang, B., Ramanis, Z., and Luck, D.J.L. (1982). Suppressor mutations in *Chlamydomonas* reveal a regulatory mechanism for flagellar function. Cell *28*, 115–124.

Huang, L. J., Durick, K., Weiner, J. A., Chun, J., and Taylor, S. S. (1997). D-AKAP2, a novel protein kinase A anchoring protein with a putative RGS domain. Proc. Natl. Acad. Sci. USA *94*, 11184–11189.

Kamiya, R., and Witman, G. B. (1984). Submicromolar levels of calcium control the balance of beating between the two flagella in demembranated models of *Chlamydomonas*. J. Cell Biol. *98*, 97–107.

Kathir, P., LaVoie, M., Brazelton, W. J., Haas, N. A., Lefebvre, P. A., and Silflow, C. D. (2003). Molecular map of the *Chlamydomonas reinhardtii* nuclear genome. Eukaryot. Cell. *2*, 362–379.

King, S. J., and Dutcher, S. K. (1997). Phosphoregulation of an inner dynein arm complex in *Chlamydomonas reinhardtii* is altered in phototactic mutant strains. J. Cell Biol. *136*, 177–191.

Koukoulas, I., Augustine, C., Silkenbeumer, N., Gunnersen, J. M., Scott, H. S., and Tan, S. S. (2004). Genomic organization and nervous system expression of radial spoke protein 3. Gene *336*, 15–23.

Lea, I. A., Widgren, E. E., and O'Rand, M. G. (2004). Association of sperm protein 17 with A-kinase anchoring protein 3 in flagella. Reprod. Biol. Endocrinol. *2*, 57.

Letunic, I., Copley, R. R., Schmidt, S., Ciccarelli, F. D., Doerks, T., Schultz, J., Ponting, C. P., and Bork, P. (2004). SMART 4.0, towards genomic data integration. Nucleic Acids Res. *32*, D142–D144.

Lohmann, S. M., DeCamilli, P., Einig, I., and Walter, U. (1984). High-affinity binding of the regulatory subunit (RII) of cAMP-dependent protein kinase to microtubule-associated and other cellular proteins. Proc. Natl. Acad. Sci. USA *81*, 6723–6727.

Luconi, M., Carloni, V., Marra, F., Ferruzzi, P., Forti, G., and Baldi, E. (2004). Increased phosphorylation of AKAP by inhibition of phosphatidylinositol 3-kinase enhances human sperm motility through tail recruitment of protein kinase A. J. Cell Sci. *117*, 1235–1246.

Malbon, C. C., Tao, J., Shumay, E., and Wang, H. Y. (2004). AKAP (A-kinase anchoring protein) domains: beads of structure-function on the necklace of G-protein signaling. Biochem. Soc. Trans. *32*, 861–864.

Mitchell, D. R. (2003). Orientation of the central pair complex during flagellar bend formation in *Chlamydomonas*. Cell Motil. Cytoskeleton *56*, 120–129.

Naaby-Hansen, S., *et al*. (2002). CABYR, a novel calcium-binding tyrosine phosphorylation-regulated fibrous sheath protein involved in capacitation. Dev. Biol. *242*, 236–254.

Nakamura, K., Fujita, A., Murata, T., Watanabe, G., Mori, C., Fujita, J., Watanabe, N., Ishizaki, T., Yoshida, O., and Narumiya, S. (1999). Rhophilin, a small GTPase Rho-binding protein, is abundantly expressed in the mouse testis and localized in the principal piece of the sperm tail. FEBS Lett. *445*, 9–13.

Newlon, M. G., Roy, M., Morikis, D., Carr, D. W., Westphal, R., Scott, J. D., and Jennings, P. A. (2001). A novel mechanism of PKA anchoring revealed by solution structures of anchoring complexes. EMBO J. *20*, 1651–1662.

Nguyen, R. L., Tam, L. W., and Lefebvre, P. A. (2005). The LF1 gene of *Chlamydomonas reinhardtii* encodes a novel protein required for flagellar length control. Genetics *169*, 1415–1424.

Pawson, T., and Scott, J. D. (2005). Protein phosphorylation in signaling–50 years and counting. Trends Biochem. Sci. *30*, 286–290.

Pazour, G. J., Sineschekov, O. A., and Witman, G. B. (1995). Mutational analysis of the phototransduction pathway of *Chlamydomonas reinhardtii*. J. Cell Biol. *131*, 427–440.

Perrone, C. A., Myster, S. H., Bower, R., O'Toole, E. T., and Porter, M. E. (2000). Insights into the structural organization of the I1 inner arm dynein from a domain analysis of the 1beta dynein heavy chain. Mol. Biol. Cell *11*, 2297–2313.

Piperno, G., Huang, B., Ramanis, Z., and Luck, D. J. (1981). Radial spokes of *Chlamydomonas* flagella: polypeptide composition and phosphorylation of stalk components. J. Cell Biol. *88*, 73–79.

Piperno, G., Ramanis, Z., Smith, E. F., and Sale, W. S. (1990). Three distinct inner dynein arms in *Chlamydomonas* flagella: molecular composition and location in the axoneme. J. Cell Biol. *110*, 379–389.

Porter, M. E., and Sale, W. S. (2000). The 9 + 2 axoneme anchors multiple inner arm dyneins and a network of kinases and phosphatases that control motility. J. Cell Biol. *151*, F37–F42.

Rawe, V. Y., Ramalho-Santos, J., Payne, C., Chemes, H. E., and Schatten, G. (2004). WAVE1, an A-kinase anchoring protein, during mammalian spermatogenesis. Hum. Reprod. *19*, 2594–2604.

Richardson, R. T., Yamasaki, N., and O'Rand, M. G. (1994). Sequence of a rabbit sperm zona pellucida binding protein and localization during the acrosome reaction. Dev. Biol. *165*, 688–701.

Rost, B., and Sander, C. (1993). Prediction of protein secondary structure at better than 70% accuracy. J. Mol. Biol. *232*, 584–599.

Rubin, R. W., and Filner, P. (1973). Adenosine 3′,5′-cyclic monophosphate in *Chlamydomonas reinhardtii*. Influence on flagellar function and regeneration. J. Cell Biol. *56*, 628–635.

Saito, T., Small, L., and Goodenough, U. W. (1993). Activation of adenylyl cyclase in *Chlamydomonas reinhardtii* by adhesion and by heat. J. Cell Biol. *122*, 137–147.

Salvador, L. M., Flynn, M. P., Avila, J., Reierstad, S., Maizels, E. T., Alam, H., Park, Y., Scott, J. D., Carr, D. W., and Hunzicker-Dunn, M. (2004). Neuronal microtubule-associated protein 2D is a dual a-kinase anchoring protein expressed in rat ovarian granulosa cells. J. Biol. Chem. 279, 27621–27632.

Schmidt, J. A., and Eckert, R. (1976). Calcium couples flagellar reversal to photostimulation in *Chlamydomonas reinhardtii*. Nature *262*, 713–715.

Sizova, I., Fuhrmann, M., and Hegemann, P. (2001). A *Streptomyces* rimosus aphVIII gene coding for a new type phosphotransferase provides stable antibiotic resistance to *Chlamydomonas reinhardtii*. Gene *277*, 221–229.

Smith, E. F. (2002). Regulation of flagellar dynein by calcium and a role for an axonemal calmodulin and calmodulin-dependent kinase. Mol. Biol. Cell *13*, 3303–3313.

Smith, E. F., and Yang, P. (2004). The radial spokes and central apparatus: mechano-chemical sensors that regulate flagellar motility. Cell Motil. Cytoskeleton *57*, 8–17.

Vijayaraghavan, S., Goueli, S. A., Davey, M. P., and Carr, D. W. (1997). Protein kinase A-anchoring inhibitor peptides arrest mammalian sperm motility. J. Biol. Chem. *272*, 4747–4752.

Wargo, M. J., and Smith, E. F. (2003). Asymmetry of the central apparatus defines the location of active microtubule sliding in *Chlamydomonas* flagella. Proc. Natl. Acad. Sci. USA *100*, 137–142.

Williams, B. D., Velleca, M. A., Curry, A. M., and Rosenbaum, J. L. (1989). Molecular cloning and sequence analysis of the *Chlamydomonas* gene coding for radial spoke protein *3*, flagellar mutation *pf*-14 is an ochre allele. J. Cell Biol. *109*, 235–245.

Witman, G. B. (1986). Isolation of *Chlamydomonas* flagella and flagellar axonemes. Methods Enzymol. *134*, 280–290.

Wong, W., and Scott, J. D. (2004). AKAP signaling complexes: focal points in space and time. Nat. Rev. Mol. Cell. Biol. *5*, 959–970.

Yang, C., Compton, M. M., and Yang, P. (2005). Dimeric novel HSP40 is incorporated into the radial spoke complex during the assembly process in flagella. Mol. Biol. Cell *16*, 637–648.

Yang, P., Diener, D. R., Rosenbaum, J. L., and Sale, W. S. (2001). Localization of calmodulin and dynein light chain LC8 in flagellar radial spokes. J. Cell Biol. *153*, 1315–1326.

Yang, P., and Sale, W. S. (2000). Casein kinase I is anchored on axonemal doublet microtubules and regulates flagellar dynein phosphorylation and activity. J. Biol. Chem. *275*, 18905–18912.